Real-world noise in hyperspectral imaging systems

Wiggins, Richard L., Comstock, Lovell E., Santman, Jeffry J.
Corning Inc., 69 Island Street, Keene, NH, USA 03431

ABSTRACT

It is well known that non-uniform illumination of a spectrometer changes the measured spectra. Laboratory calibration of hyperspectral imaging systems is careful to minimize this effect by providing repeatable, uniform illumination[1,2]. In hyperspectral measurements the real world images result in non-uniform illumination. We define the resulting variation as real-world noise and we compare real-world noise to other noise sources. Both in-flight performance and calibration transfer between instruments degrade significantly because of real-world noise.

Keywords: **Keywords:** hyperspectral, imaging, spectroscopy, spectral noise

1. INTRODUCTION

Hyperspectral imaging systems are designed to measure the spectral content of each pixel of an image. The measurements are used in developing an algorithm to classify objects and later to identify objects with that algorithm. Minimal success requires reproducible measurements on a single instrument. Transferring an algorithm between systems requires reproducible measurements on a set of instruments.

Much design and expense is used to reduce the noise sources that limit reproducibility in hyperspectral imaging systems.[3,4] Similar efforts apply to the development of algorithms that encompass all of the scene variations observed by the system.[5]

The noise that originates in the coupling of the scene variations into the system is generally ignored. We define this noise as real world noise because it is not observed during laboratory measurements of the system. We examine this noise in a hyperspectral imaging system based on a spectrometer, but real world noise exists in all hyperspectral systems. We estimate that real world noise has significant magnitude. We examine mitigation.

2. A SIMPLE EXAMPLE

Consider the hyperspectral imaging system based on the 3-pixel spectrometer shown in figure 1. The scene is imaged on the entrance slit of the spectrometer. In the spectrometer the entrance slit is imaged on the focal plane. The focal plane has three pixels centered at red = 650 [nm], yellow = 550 [nm], and blue = 450 [nm]. We have developed the calibration shown in figure 2 for objects in the town of Simpleville. Simpleville consists of 650 [nm] red roofs, 450 [nm] blue cars, 500 [nm] green cars, and 550 [nm] yellow cars. The green cars are identified by their equal illumination of the blue and yellow pixels. The other objects give unique signals from single pixels.

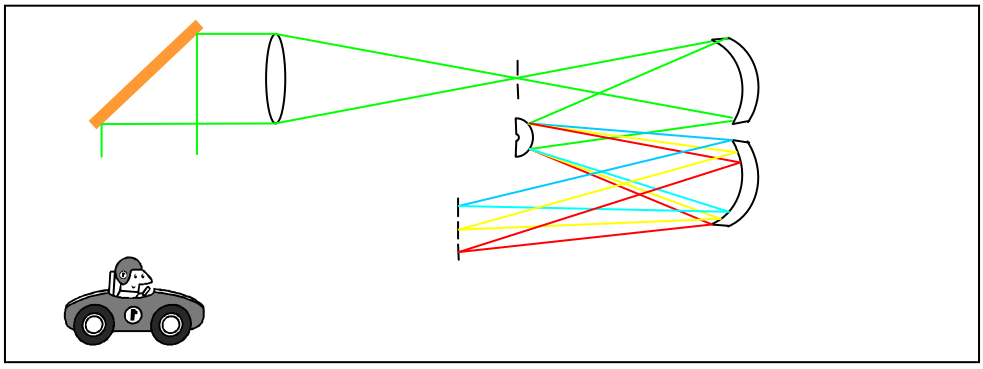

Figure 1. An Offner spectrometer based hyperspectral imaging system

Airborne Intelligence, Surveillance, Reconnaissance (ISR) Systems and Applications VIII,
edited by Daniel J. Henry, Beato T. Cheng, Dale C. Linne von Berg, Darrell L. Young, Proc. of SPIE
Vol. 8020, 802004 · © 2011 SPIE · CCC code: 0277-786X/11/$18 · doi: 10.1117/12.884886

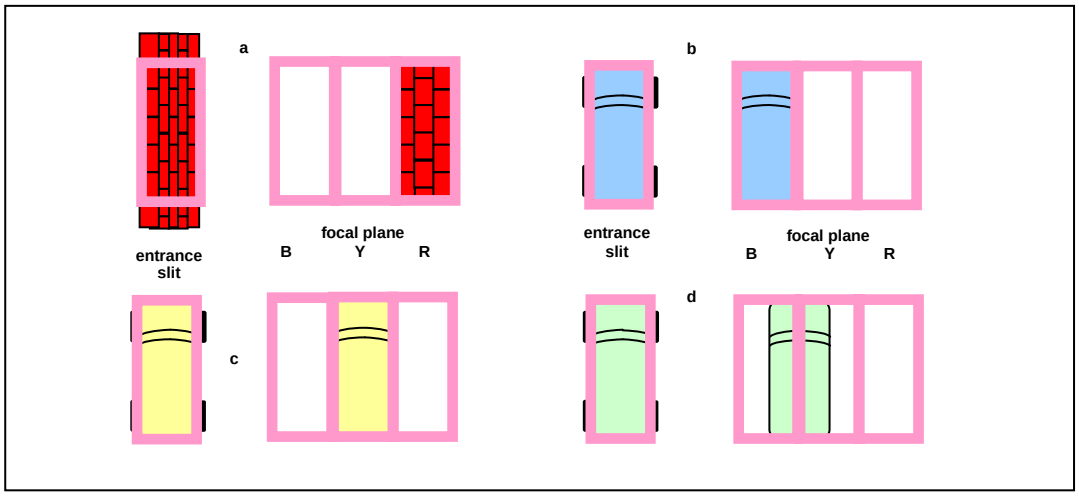

Figure 2. Simpleville hyperspectral scenes. In (a) the 650 [nm] red roof at the entrance slit is imaged onto the red pixel. In (b) the 450 [nm] blue car is imaged on the blue pixel. In (c) the 550 [nm] yellow car is imaged on the yellow pixel. In (d), the 500 nm green car is imaged at the 500 nm position. The image is partly on the blue pixel and partly on the yellow pixel.

What happens if there are two objects imaged on the entrance slit? Figure 3 shows the entrance slit split between the green car and the red roof. In this configuration the car only generates a blue signal so it is identified as blue.

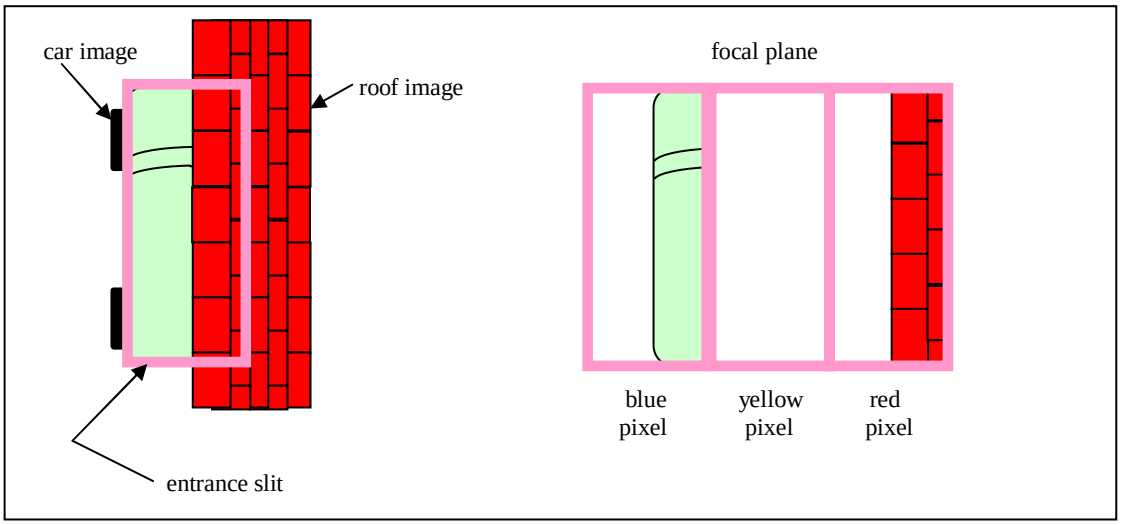

Figure 3. The spectrometer images the half of the red roof at the entrance slit onto half of the red pixel. The red roof is still identified as red. The spectrometer images the half of the green car at the entrance slit onto half of the blue pixel. The car-half that was imaged onto the yellow pixel in Fig.2d is not present.

The Simpleville example shows the mechanism of real world noise. The importance of real world noise can be determined by simulation. Simulation can estimate of the magnitude of real world noise compared to other noise sources. Simulation can also determine if real-world noise is highly correlated and easily removed by analysis.

3. SIMULATION OF THE IRRADIANCE AT THE FOCAL PLANE

The spectral irradiance at the focal plane of a spectrograph, $E_\lambda'[\lambda, x', y']$ in a hyperspectral imaging system is related to the spectral irradiance of the entrance slit $E_\lambda[\lambda, x, y]$ by

$$E_\lambda'[\lambda, x', y'] = \iint_{slit} E_\lambda[\lambda, x, y] \cdot R[x.x', y, y', \lambda] \cdot dxdy \quad (1)$$

where $R[x, x', y, y', \lambda]$ is the instrumental transfer function of the spectrograph
x, y are the vertical and horizontal coordinates in the entrance slit plane
x', y' are the vertical and horizontal coordinates in the focal plane
spectral dispersion is in the horizontal plane

Consider an ideal spectrograph with no losses, perfect imaging, linear dispersion, and unity magnification. The spectrograph transfers light of wavelength, λ_0, from the entrance slit center, y = 0 , to the center of the exit focal plane, y' =0, with dispersion, D. Then, the instrumental response function, R, for the spectrograph is

$$R[y, y', \lambda] = \delta[y' - y + D(\lambda_0 - \lambda)] \quad (2)$$

where the dispersion, typically nanometers per millimeter, is D.

There is no dependence on vertical position, so x' = x and the spectral irradiance at the focal plane becomes

$$E'_\lambda[\lambda, x', y'] = \int_{y\min}^{y\max} E_\lambda[\lambda, x', y] \cdot Rinst[y, y', \lambda] \cdot dy . \quad (3)$$

From equations (2) and (3) and knowledge of the spectral irradiance at the entrance slit, it is possible to calculate the spectral irradiance at the exit slit.

4. PROPERTIES OF REAL WORLD NOISE

The lodgepole pine spectra in the USGS Spectral Library are typical of airborne spectral measurements. The data originates from the AVIRIS spectrometer and has approximately 10 [nm] resolution. The set of eleven spectra shown in Figure 4 are derived from the original data by 3-point-spline interpolated from the original data onto a linear wavelength scale having 2 [nm] spacing. In addition, normalizing the average intensity of each spectrum removes gross illumination variation.

The spectra are the basis for simulating the output of a spectrometer with a 20 [nm] bandpass. 20 nm is a reasonable simulation choice. During the design of a hyperspectral imaging system the spectral bandwidth is selected to approximate the linewidths of the spectral lines that are observed. The narrowest features in the lodgepole pine spectra have 50 [nm] bandwidths.

Two different entrance slit spectral irradiances are used in simulation. A uniform irradiance simulates measurements without real world noise. This irradiance is used for each of the original spectra. Irradiance over half of the slit with a randomized origin simulates measurements with real world noise. This irradiance is applied to the average spectrum only. Half-slit irradiance is a reasonable simulation choice. During the design of a hyperspectral imaging system the width of the spectrometer entrance slit is selected to approximate the sizes of the interesting features in the image. Many real systems present images to the entrance slit that have resolutions ten times smaller than the entrance slit.

Simulation uses equations (2) and (3). The integration of equation (3) is approximated by a summation over tenth-slit increments, corresponding to the 2[nm] granularity of the interpolated lodgepole pine irradiance spectra.

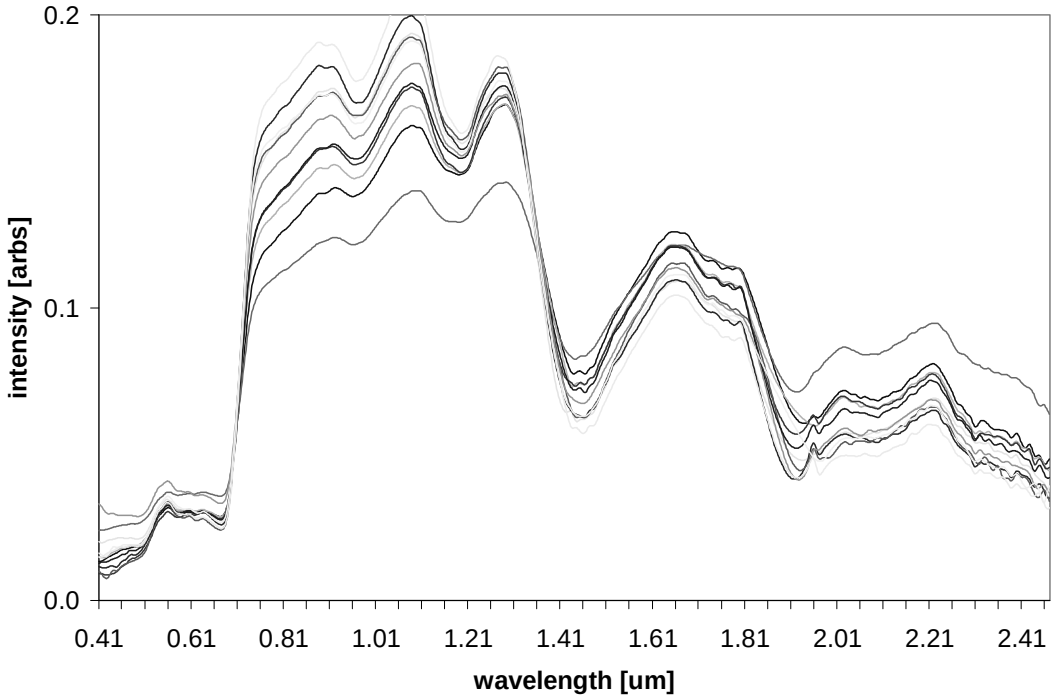

Figure 4. Eleven spectra of lodgepole pine, 3-point-spline interpolated at 2nm and normalized.

The standard deviation at each wavelength is used as a measure of noise. The uniform irradiance spectra span the range of variations in the original data set. The real-world irradiance spectra are the result of applying real world noise to a single average spectrum. Figure 5 shows the comparison. The variation induced by real world noise is about 7% of the original variation in the data set.

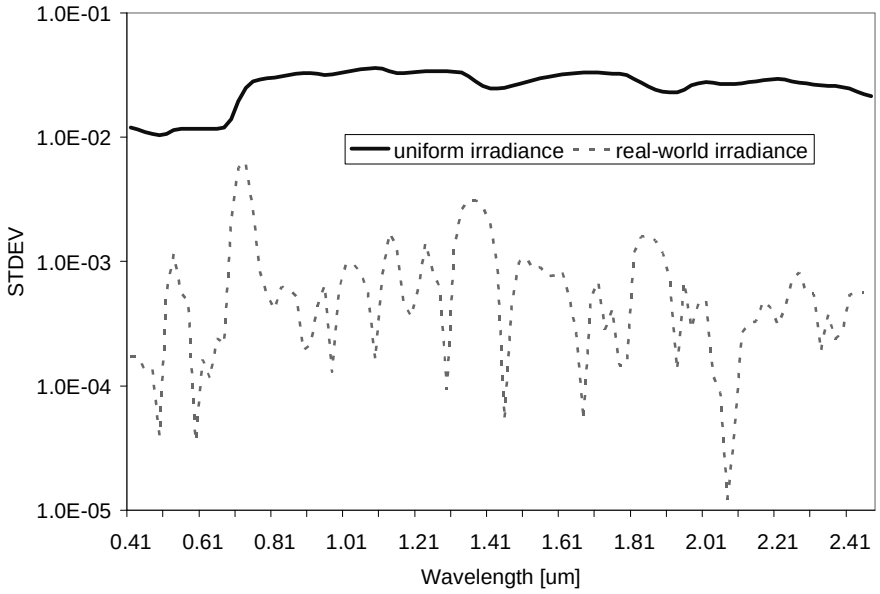

Figure 5. Variation in original data set and variation induced by real-world noise.

While real-world noise has significant magnitude, if it is highly correlated across the spectrum it will be easily removed. Principle components analysis (PCA) is used as a measure of spectral correlation in the data. PCA extracts the largest correlated variation in a data set, and then extracts successively smaller correlated variations.[7] For use in PCA analysis a simulation set was created that combined the variations between the original spectra and variations induced by real-world irradiance of the entrance slit. In the new data set, random real-world irradiance was applied to each of the spectra in the original data set. The results are shown in figure 6.

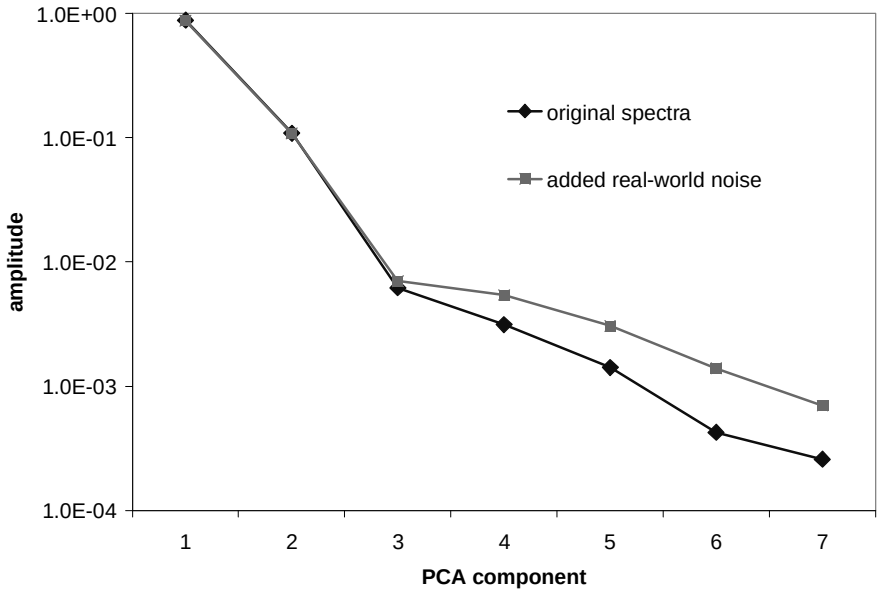

Figure 6. Amplitudes of PCA components for original data set and for data set with real-world variations included.

After the third PCA component, the analysis is less successful at finding correlations in the data that includes real-world noise. The real world noise is not highly correlated and is not easily removed by analysis.

5. REAL WORLD NOISE AND REAL DETECTORS

The simulations above have ignored any non-uniformity of response in the focal plane array. Figure 7 shows a measurement of this non-uniformity in a CCD detector taken from Kavaldjiev and Ninkov[8].

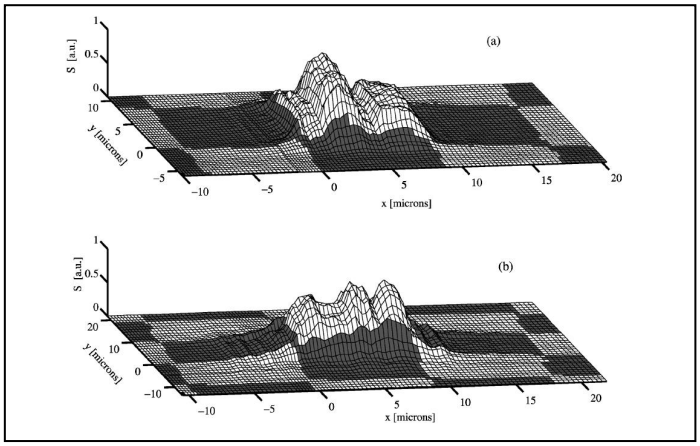

Figure 7. CCD pixel response uniformity at two wavelengths from Kavaldjiev and Ninkov[8]

Non-uniformity in the detector pixels will amplify the effect of real-world noise that has been previously simulated. In hyperspectral systems without dispersion such as filter based systems, the non-uniformity of the detector pixels combine with image features to create real-world noise.

The real-world noise connected to pixel non-uniformity will also inhibit transfer of classification algorithms between instruments. The standard calibration methods used to make spectrometers appear identical rely on uniform illumination. The spectral shifts introduced by real-world noise are not calibrated out in this process.

6. MITIGATION OF REAL-WORLD NOISE

Mitigation of real world noise requires creating uniform illumination across the slit width. The simplest mitigation of real-world noise is a design in which image features on the scale of the entrance-slit width are not resolved. Defocus of the image on the entrance slit may be satisfactory. However, the loss of image resolution is frequently unacceptable. An ideal method would provide homogenization on the scale of the slit width, conservation of etendue, wavelength independence, and good transmission.

In trying to improve hyperspectral imaging Corning is actively investigating methods of real-world noise mitigation, and is seeking patents in the area. One promising method is the use of arrays of optical waveguides as homogenizers. The optics of single waveguides as MTF attenuation elements is well developed.[9] Corning regularly manufactures IR waveguides on a scale of tens of microns for its customers. Figure 8 pictures one of Corning's single waveguides.

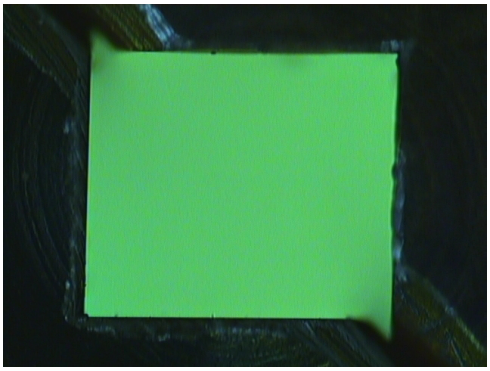

Figure 8. A 0.08 [mm] square all reflective Comstock waveguide illuminated at left rear only

7. CONCLUSION

Real-world noise is a significant noise source in hyperspectral imaging. Real-world noise can be simulated to the extent that the instrumental transfer function of the spectrometer-fpa system is understood. Real-world noise is caused by the interaction of the spectrometer with the non-uniform illumination provided by the real world, but it can be mitigated by instrumental design measures.

REFERENCES

[1] Chrien, T.G., Green, T.O., and Eastwood, M.L., "Accuracy of the spectral and radiometric laboratory calibration of the Airborne Visible/Infrared Imaging Spectrometer," Proc. SPIE 1298, 37-49 (1990)

[2] Zadnik, J., Guerin, Moss, R.D., Orbeta, A., Dixon R., Simi, C., Dunbar S., and Hill, A., "Calibration Procedures and Measurements for the COMPASS Hyperspectral Imager," Proc. SPIE 5425, 182-188 (2004)

[3] Bender, H.A., Mouroulis, P.Z. and Green, R.O., and Wilson, D.W., "Optical design, performance and tolerancing of next-generation airborne imaging spectrometers," Proc. SPIE 7812, 1-12 (2010)

[4] Mouroulis, P.Z. and Green, R.O., "Optical design for high-fidelity imaging spectrometry," Proc. SPIE 4829, 1048-1049 (2003)

[5] Mariano, A.V., and Grossmann, J.M., "Hyperspectral material identification on radiance data using single-atmosphere or multiple-atmosphere modeling," Journal of Applied Remote Sensing, Vol. 4, 043563 (2010)

[6] Clark, R.N., Swayze, G.A., Wise, R., Livo, E., Hoefen, T., Kokaly, R., Sutley, S.J., 2007 “USGS digital spectral library splib06a”, http://speclab.cr.usgs.gov/spectral.lib06/
[7] Shlens, J., “A Tutorial on Principal Component Analysis”, http://www.snl.salk.edu/~shlens/pca.pdf, (2009)
[8] Kavaldjiev, D., and Ninkov, Z., " Subpixel sensitivity map for a charge-coupled device sensor," Opt. Eng. 37(3) 948–954 (March 1998).
[9] Cheng, Yi-Kai and Chern, Jyh-Long “Irradiance formations in hollow straight light pipes with square and circular shapes,” J. Opt. Soc. Am. A, 23(2) 427-434 (2006)